Bioactive Materials 6 (2021) 880–889

Contents lists available at ScienceDirect

Bioactive Materials

journal homepage: http://www.keaipublishing.com/biomat

Significant difference between sirolimus and paclitaxel nanoparticles in anti-proliferation effect in normoxia and hypoxia: The basis of better selection of atherosclerosis treatment

Youlu Chen[a,1], Yong Zeng[b,1], Xiaowei Zhu[a,c], Lifu Miao[d], Xiaoyu Liang[a], Jianwei Duan[a], Huiyang Li[a], Xinxin Tian[a], Liyun Pang[a], Yongxiang Wei[b,**], Jing Yang[a,e,*]

[a] Tianjin Key Laboratory of Biomaterial Research, Institute of Biomedical Engineering, Chinese Academy of Medical Science and Peking Union Medical College, Tianjin, 300192, PR China
[b] Beijing Institute of Heart Lung and Blood Vessel Disease, Beijing Anzhen Hospital, Capital Medical University, Beijing, 100029, PR China
[c] Henan Center for Patent Examination and Cooperation of the Patent Office of the State Intellectual Property Office, Henan, 450002, PR China
[d] Heart Center, The First Hospital of Tsinghua University, Beijing, 100016, PR China
[e] Biomedical Barriers Research Center, Institute of Biomedical Engineering, Chinese Academy of Medical Sciences & Peking Union Medical College, Tianjin, 300192, PR China

ARTICLE INFO

Keywords:
Atherosclerosis
Sirolimus
Paclitaxel
Hypoxia
HIF-1α
Glycolysis

ABSTRACT

Compared with paclitaxel, sirolimus has been more used in the treatment of vascular restenosis gradually as an anti-proliferative drug, but few basic studies have elucidated its mechanism. The anti-proliferative effects of sirolimus or paclitaxel have been demonstrated by numerous studies under normoxia, but few studies have been achieved focusing hypoxia. In this study, porcine carotid artery injury model and classical cobalt chloride hypoxia cell model were established. Sirolimus nanoparticles (SRM-NPs), paclitaxel nanoparticles (PTX-NPs) and blank nanoparticles (Blank-NPs) were prepared respectively. The effect of RPM-NPs on the degree of stenosis, proliferative index and the expression of PCNA after 28 days of porcine carotid artery injury model was evaluated. Compared with saline group and SRM groups, SRM-NPs group suppressed vascular stenosis, proliferative index and the expression of PCNA ($P < 0.01$ and $P < 0.05$). Endothelial cell (EC) and smooth muscle cell (SMC) were pre-treated with cobaltous chloride, followed by SRM-NPs, PTX-NPs, Blank-NPs or PBS control treating, the effects on cell proliferation, HIF-1 expression and glycolysis were detected. SRM-NPs could inhibit EC and SMC proliferation under hypoxia, while PTX-NPs couldn't ($P < 0.001$). Significant differences between sirolimus and paclitaxel NPs in anti-proliferation effect under normoxia and hypoxia may due to the different inhibitory effects on HIF-1α expression and glycolysis. In conclusion, these results suggest that sirolimus can inhibit the proliferation of hypoxic cells more effectively than paclitaxel. These observations may provide a basis for understanding clinical vascular stenosis therapeutic differences between rapamycin and paclitaxel.

1. Introduction

Cardiovascular disease (CVDs) remains the leading cause of death worldwide [1]. Atherosclerosis is at the root of the most life-threatening CVDs [2]. Percutaneous coronary intervention (PCI) reopens the coronary arteries by balloon or stent and keeps the arteries that have been narrowed by arteriosclerosis unobstructed [3]. However, restenosis often occurs due to abnormal cell proliferation, and then anti-proliferative drugs are used to reduce cell proliferation and alleviate vascular stenosis [4,5]. Both sirolimus and paclitaxel are commonly used anti-proliferative drugs, but in clinical studies (such as RAVEL, SIRIUS, TAXUS trials and so on), sirolimus-eluting stent (SES) is superior to paclitaxel eluting stent (PES) in restenosis rate [6,7]. Due to the advantages of sirolimus, the second-generation drug-eluting stent carries

Peer review under responsibility of KeAi Communications Co., Ltd.
* Corresponding author. Tianjin Key Laboratory of Biomaterial Research, Institute of Biomedical Engineering, Chinese Academy of Medical Science and Peking Union Medical College, Tianjin, 300192, PR China.
** Corresponding author.
E-mail addresses: weiyongxiang@vip.sina.com (Y. Wei), yangjing37@hotmail.com (J. Yang).
[1] These authors made equal contributions to this work.

https://doi.org/10.1016/j.bioactmat.2020.09.005
Received 3 June 2020; Received in revised form 8 September 2020; Accepted 9 September 2020

sirolimus or its derivatives [8].

Sirolimus replaced paclitaxel gradually, but few studies have been done to elucidate the mechanism. In previous studies, sirolimus, developed as an mTOR inhibitor and antibiotic with potent immunosuppressive properties, inhibits the various processes of restenosis cascade, and it can also regulate cell proliferation cycle arrest at G1/S phase [9]. Paclitaxel, developed as an anti-neoplastic drug, inhibits the disassembly of micro-tubules which blocks mitosis progression and thus G2/M-phase arres [10]. To some extent, both sirolimus and paclitaxel inhibited cell proliferation. But these studies are usually carried out under normoxia. In fact, advanced vascular stenosis shows areas of severe hypoxia and is rich in angiogenesis [11]. These microenvironments have been neglected, and further researches could begin with hypoxic microenvironment.

Differences of anti-proliferation between sirolimus and paclitaxel may relate to hypoxia microenvironment of atherosclerosis, because there are a series of changes in cells during hypoxia. Firstly, HIF-1α as the main regulator of cellular response to hypoxic environment will be expressed in Hypoxia microenvironment quickly [12]. Then, HIF-1α promotes the development of atherosclerosis through promoting the expression of vascular endothelial growth factor (VEGF), proliferation of endothelial cell (EC) and smooth muscle cell (SMC), glycolysis and so on [13]. Therefore, HIF-1α expression and glycolysis under hypoxia will reflect the anti-proliferation ability of drugs from another side [14].

Both sirolimus and paclitaxel are lipid-soluble drugs. The combination of nanotechnology could improve solubility, enhance bioavailability and prolong action cycle of them [15]. Therefore, in this study, 3S-PLGA was used as carrier to prepare paclitaxel and sirolimus nano-drug delivery system. The effects of sirolimus and paclitaxel on EC and SMC under normoxic and hypoxic microenvironment were compared in terms of cell proliferation, HIF-1α expression and glycolysis, which may provide a possible theoretical basis for the selection of therapeutic drugs for vascular restenosis. Hopefully, this study will stimulate more thinking and research, and contribute to the treatment of vascular restenosis in the future.

2. Materials and methods

2.1. Materials

Cobalt (II) chloride hexahydrate was purchased from Sigma (St. Louis, MO, USA); *Anti*–HIF–1α, Anti-beta Actin, IgG H&L (DyLight 488) and IgG H&L (HRP) were obtained from Abcam (Cambridge, UK); Paraformaldehyde, DAPI, MTT, RIPA Lysis Buffer, 5 × SDS-PAGE Sample Loading Buffer, 20 × TBST buffer, ECL Western Blotting Substrate and Color Mixed Protein Marker were from Solarbio (Beijing, China); SDS-PAGE gel preparation kit and Lyso-Tracker were bought from Beyotime (Jiangsu, China).

2.2. Animal experiments

Chinese Experimental Mini-pigs (CEMPs) (weight 20–23 kg, 5–7 month) were purchased from China Agricultural University Animal Center (Beijing, China). The Administrative Committee on Animal Research in the Chinese Academy of Medical Science approved all the protocols for animal experiments. Also, all the animal experiments were performed in compliance with the Guiding Principles for the Care and Use of Laboratory Animals, Peking Union Medical College, China.

2.3. Preparation of NPs

Paclitaxel (or sirolimus) was encapsulated in 3s-PLGA by ultrasonic emulsification and solvent evaporation technology to prepare SRM-NPs and PTX-NPs. The specific process is as follows: first, weigh 30 mg paclitaxel (or sirolimus) and 100 mg 3S-PLGA accurately, and add 1.5 mL dichloromethane to dissolve them. Then, prepare 1% PVA (w/V) aqueous solution, drop the solution above into 1% PVA aqueous solution under constant ultrasound (shear force 30%, 10 min, ice bath). At that time, paclitaxel (or sirolimus) was encapsulated in the NPs formed by 3s-PLGA and nanoparticle suspension was formed. Next, the nanoparticle suspension was stirred for 2 h at room temperature to remove the volatile dichloromethane. Then, the suspension was centrifuged and washed with distilled water twice to remove PVA (23,000 r/min, 4 °C, 30min). The preparation methods of Blank-NPs and coumarin 6-NPs were similar to the above steps. The differences were that coumarin 6-NPs were prepared with 8 mg coumarin 6 instead of paclitaxel (or sirolimus), and Blank-NPs were not loaded any drugs.

2.4. Size distribution, zeta potential, stability and morphology of NPs

Take 2 mL of Blank-NPs, SRM-NPs and PTX-NPs suspensions, and use dynamic light scattering (DLS) method to measure the average particle size, particle size distribution and zeta potential on zeta sizer nano ZS (Malvern instruments, UK).

Keep the Blank-NPs, SRM-NPs and PTX-NPs suspensions that have been tested for particle size, and measure the particle size every 6 d to test the stability of NPs.

100 μl Blank-NPs, SRM-NPs and PTX-NPs suspensions were uniformly dispersed in 1 mL distilled water and dropped on the copper mesh. After drying, the morphology of *NPs* was observed by transmission electron microscopy (TEM). (h-6009iv, Hitachi).

All measurements are made in triplicate. The average particle size is represented by the volume average diameter, and the reported value is represented by the average ± standard deviation ($n = 3$).

2.5. Drug loading, encapsulation and releasing of NPs

Weigh 2.5 mg of drug-loaded NPs accurately, suspending them with 4 mL PBS(1 mol/L) and placing them in constant temperature shaking table for release experiment (37 °C, 130 r/min). The release solution was taken out on 1 d, 3 d, 5 d, 8 d, 12 d, 16 d and 20 d respectively, and the same amount of fresh PBS was added to replace the release solution. After the release liquid was extracted by dichloromethane, the drug content was determined by High performance liquid chromatography (HPLC), and the cumulative release curve was drawn. The cumulative release curve is calculated as follows.

After weighing 5 mg NPs accurately, the NPs were completely dissolved in 1 mL dichloromethane. Volatilize dichloromethane in the fume hood until the solution was completely volatilized. Then, adding 1 mL acetonitrile to dissolve released drugs, the content of drugs was determined by HPLC. The calculation formula of drug loading is as follows.

Paclitaxel (or sirolimus), which is not encapsulated in NPs, would remain in the supernatant solution. Therefore, in the preparation of NPs, the supernatant obtained after the first centrifugation needs to be preserved for the detection of encapsulation efficiency. The calculation formula of enveloping rate is as follows.

HPLC: 20 μL samples were injected into a reverse C18 column (150 4.6 mm, 5 m) with a mobile phase ratio of acetonitrile: water (50:50, v: v) at a flow rate of 1 mL/min. The absorption was determined by UV at $\lambda = 227$ nm (PTX) or $\lambda = 278$ nm (SRM). The results were expressed as average ± standard deviation ($n = 3$).

$$Cumulative\ release\ (\%) = \frac{Cumulative\ release\ of\ drug}{Total\ mass\ of\ loaded\ drug} \times 100\%$$

$$Drug\ loading\ (\%) = \frac{Total\ mass\ of\ drug}{Total\ mass\ of\ NPs} \times 100\%$$

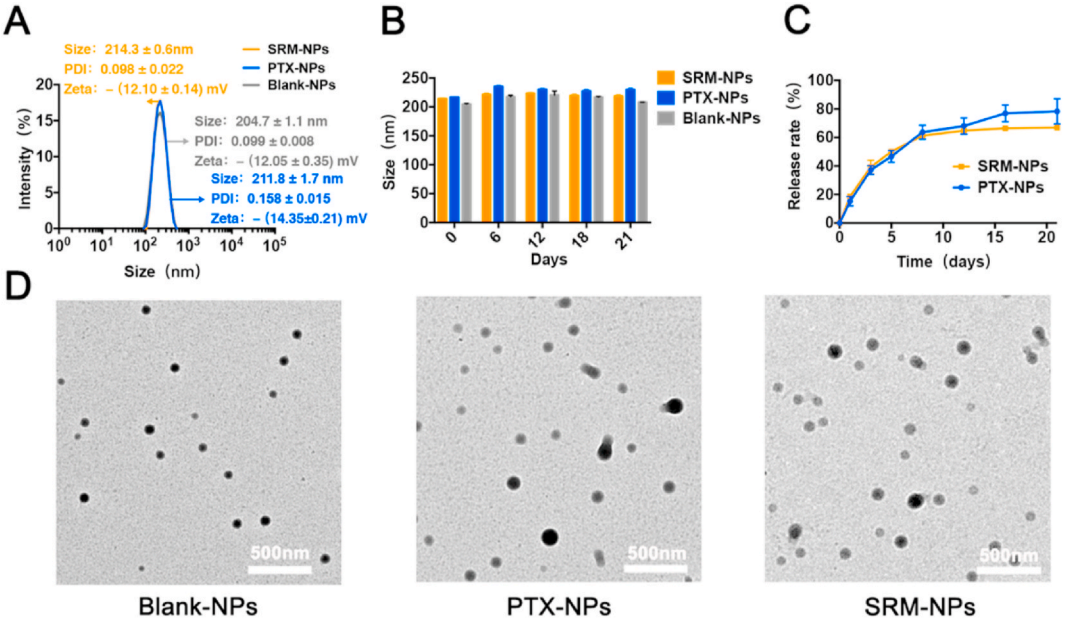

Fig. 1. Characterization of Blank-NPs, SRM-NPs and PTX-NPs in vitro. (A) The particle size of them was (204.7 ± 1.1) nm, (214.3 ± 0.6) nm and (216.9 ± 0.6) nm, the PDI value was (0.099 ± 0.008), (0.098 ± 0.022) and (0.129 ± 0.046), and the surface potential was - (12.05 0.35) mV, - (12.10 ± 0.14) mV and - (14.35 ± 0.21) mV. (B) Stability test showed that the Blank-NPs, SRM-NPs and PTX-NPs had good stability within 21 d. (C) In *vitro* release results showed that the system could achieve relatively similar release of SRM-NPs and PTX-NPs. (D) Typical images of three kinds of nanoparticles under TEM, NPs were spherical.

$$\textit{Encapsulation rate}\ (\%) = \frac{\textit{Total mass of drug—drug mass in supernatant solution}}{\textit{Total mass of drug}} \times 100\%$$

2.6. Cellular uptake of NPs

Cells were inoculated in a confocal dish at a density of 1×10^5 cells per well, with 1 mL medium per dish. After 24 h of culture, Coumarin-NPs were added, and the NPs were added to the confocal dish at a concentration of 100 μg/mL. At 24 h, the culture medium was gently sucked out, and each dish was washed with 1 mL PBS three times. Each well was filled with 500 μL 4% paraformaldehyde for 20 min at RT. Removed polyformaldehyde gently, then each dish was washed three times by PBS, 5 min each time. After that, used 400 μL Lyso-Tracker Red to incubate overnight. DAPI dye solution of 300 μL per dish was used for nuclear staining at RT for 5 min, each dish was washed with 1 mL PBS three times, 5 min each time. Then 300 μL PBS was added to each dish, and the distribution of NPs in cells was observed under a laser confocal microscope.

2.7. The curative effect of SRM-NPs on swine

Before surgery 1 day, Chinese Experimental Mini-pigs (CEMPs) (weight 20 to 23 Kg) were administrated aspirin (325 mg) till were sacrificed. CEMPs were anesthetized using Ketamine(15 g/kg) and Atropine (0.5 mg), then were binded on operating table with the real–time dynamic ECG monitoring system. At groin, through a midline neck incision the right common, external and internal carotid arteries were exposed and swilled with heparin saline. The endothelium of the right common carotid artery was distended by Judkin catheter. The mid and distal portions were temporarily tied off to form a close segment. Twenty-eight CEMPs were divided by four groups, group A B C D were separately infused different therapeutic solution, A is saline, B is blank NPs, C is SRM, D is SRM-NPs, therapeutic solution was infused into the temporarily closed left common carotid segment using the Dispatch local delivery infusion balloon under 1 ATM pressure for 10 min before the ties were removed and the flow was restored, the left external carotid artery was ligated and the skin was closed. Penicillin were administered 3 days after surgery. Morphometric analysis was performed on the H&E-stained sections and immunohistochemical staining sections of swine carotid arteries that were collected on day 28 after balloon angioplasty. Histologically, the degree of stenosis, proliferative index and the expression of PCNA were tested by IPP4.0 true-color image processing software and image j software.

2.8. Cytocompatibility and cell proliferation inhibition of NPs

EC (or SMC) were seeded into 96-well plate in 100 μL medium (5×10^3 cells/well) under normoxia. EC (or SMC) were cultured for 24 h to achieve 90% fusion. NPs were set in 6 parallel wells of each group (concentrations were 0.01, 0.05, 0.1, 0.5, 1, 5, 10, 50, 100 μg/mL, respectively), The negative control group cells were added with the same amount of serum-free medium. Cell viability was analyzed by MTT (5 mg/mL) assay after cultured 24 h, 48 h and 72 h. The OD value of each well was detected at the wavelength of 490 nm.

Construction of hypoxia environment: EC (or SMC) were seeded into 96-well plate in 100 μL medium (5×10^3 cells/well). EC (or SMC) were cultured for 24 h to achieve 90% fusion. Then, EC (or SMC) were cultured for 24 h in a serum-free medium containing 200 μmol/L cobal tdichloride. And the concentrations of added NPs were 1, 5, 10, 50, 100, 500, 1000, 2000 μg/mL, respectively. The process of other experiments and detection is the same as normoxia.

$$\textit{Cell viability}\ (\%) = \frac{\textit{OD value of NPs group}}{\textit{OD value of negative control group}} \times 100\%$$

2.9. Cellular immunofluorescence

The cells were immobilized with 4% paraformaldehyde for 20 min and washed by PBS for 3 times. Then, 0.5% Triton X-100 was used to infiltrate for 20 min at RT, and was rinsed 3 times by PBS. After 30 min of blocking with 300 μL goat serum (5%) at RT. Then 300 μL primary antibody (200 × dilution) was added to incubate at 4 °C overnight and washed with PBS for 3 times. The cells were incubated with fluorescent

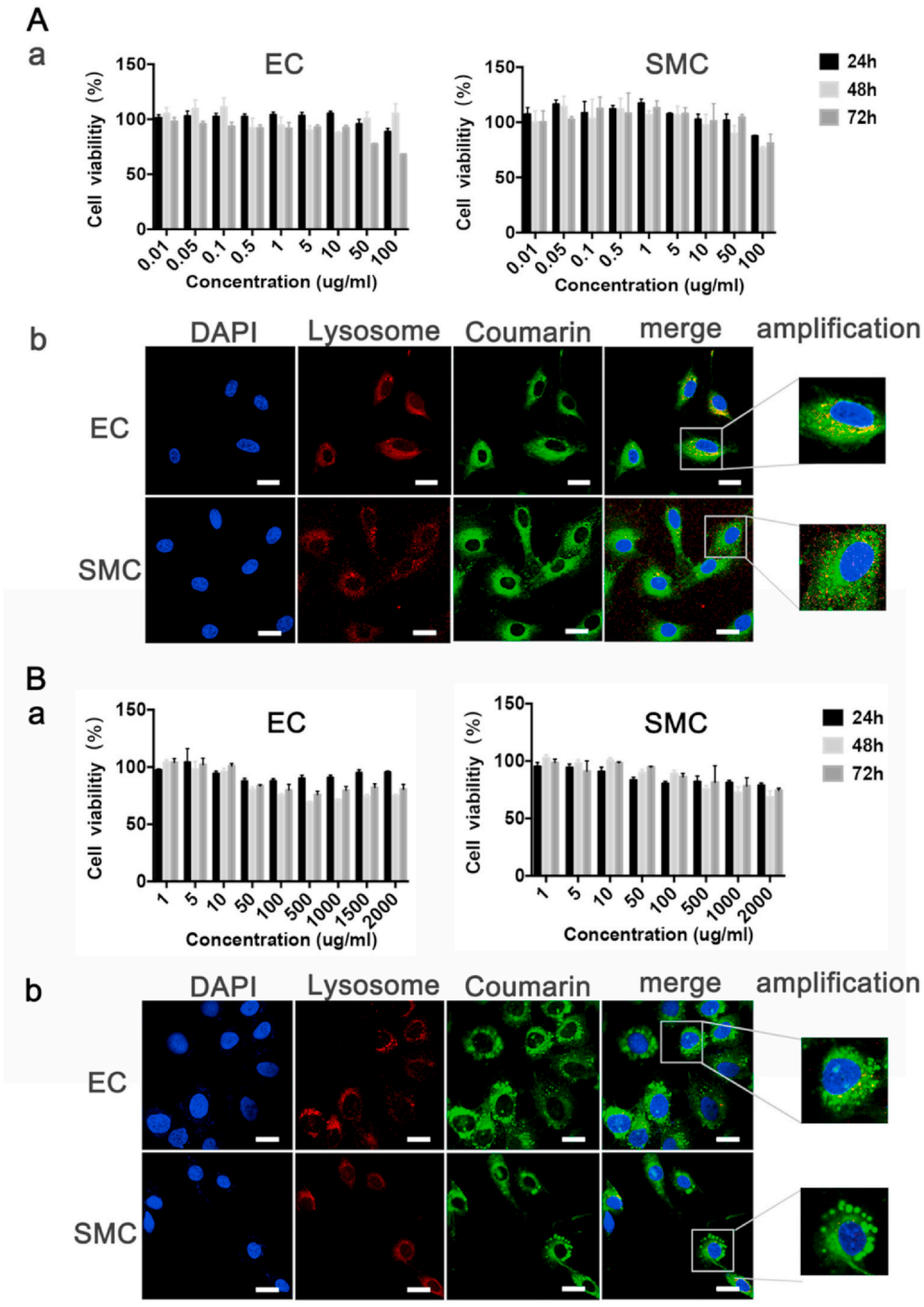

Fig. 2. Cytocompatibility of Blank-NPs and uptake of Coumarin-6 NPs by cells. Cytocompatibility testing and cell uptake of Blank-NPs were detected. Within 24 h–72 h, Blank-NPs had almost no inhibitory effect on the growth of EC and SMC in normoxia (A, a) and hypoxia (B, a), and the cell survival rate was basically above 75%. Coumarin-6 NPs can be successfully swallowed into cells by EC and SMC under normoxia (A, b) and hypoxia (B, b), and lysosomal escape has been achieved. (A,b & B,b)The white bars represent 20 μm, blue stands for DAPI and green represents coumarin 6. (For interpretation of the references to color in this figure legend, the reader is referred to the Web version of this article.)

antibody (200 × dilution) at 37 ˚C for 1 h and washed by PBS for 3 times. The cells were incubated with 300 μL DAPI for 5 min, washed for 3 times with PBS, and then 500 μL PBS was added. They were observed and photographed under a confocal laser microscope.

2.10. Western blotting

Total protein was extracted and quantified. The protein samples were diluted with dilution buffer and denatured at 95 ˚C or above for 10 min. Samples were added into SDS-PAGE colloidal pore and electrophoresis was carried out at 80 V 2 h. After membrane metastasis (90 V, 60 min), 2% BSA was used to block the nonspecific site for 1 h. After 4 rinses with TBST, the primary antibodies (200 × dilution) were incubated overnight at 4 ˚C. TBST was used to wash the second antibody for four times and incubate the second antibody (5000 × dilution) for 1 h at 37 ˚C. After cleaning four times with TBST and reacting for 1 min, the developer was added to the imaging system for exposure and image acquisition.

2.11. Inhibition of cell glycolysis

The cells were seeded into cell plate with 100 μL medium, the density of cells was 5×10^5/mL. Then the cells were adhered to the cell plate wall for 4 h and the culture medium was discarded. Cells were incubated overnight at high and low doses of NPs (1000 μg/mL and 100 μg/mL) under hypoxia conditions. In addition, adding 1 mL Calibrant to each hole of probe plate, then insert the probe, incubating in 5% CO_2 incubator at 37 ˚C overnight. Preheating the working

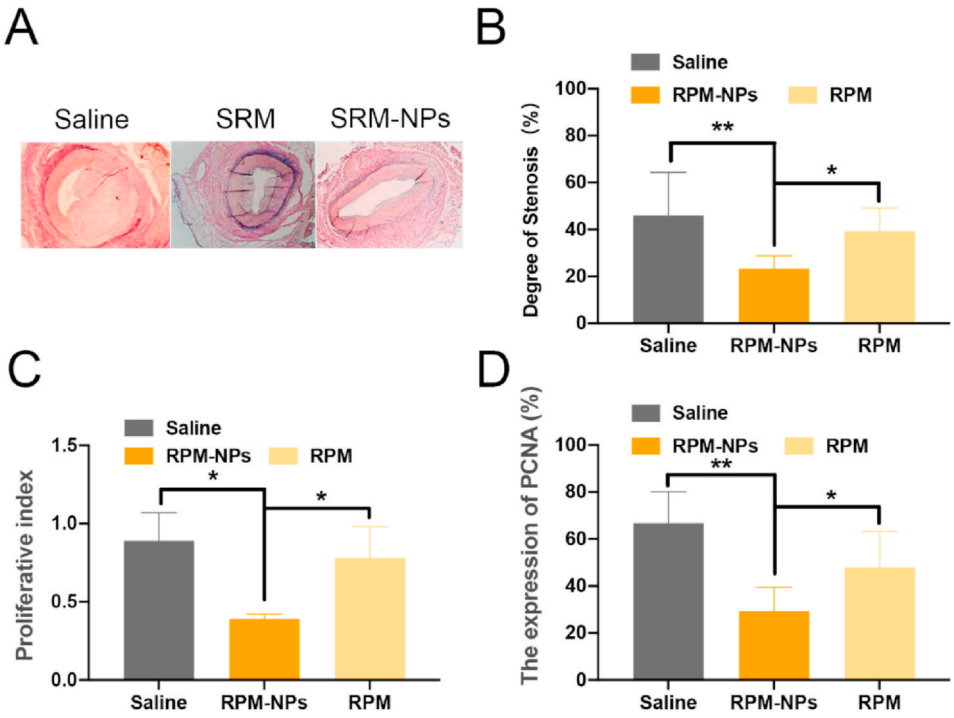

Fig. 3. The result of histopathological evaluation. (A), the condition of intima hyperplasia; (B), degree of stenosis; (C), proliferative index; (D), the expression of PCNA.

solution (PH 7.4, 5 mM glutamine) and removing the old medium containing NPs in cell plate. Washing cells with 1 mL working solution twice and adding 500 μL working fluid to each hole of cell plate. Cells were observed under a microscope and are required to adhere to the wall. After that, the cell plate was placed at 37 ˚C without CO_2 incubator for 1 h. Glucose, Oligomycin and 2-DG were added to the A, B and C pores of the probe plate in sequence. Put the probe plate above the cell plate for about half an hour at 37 ˚C without CO_2 incubator. After incubation, remove the probe plate tray and cover. The cell culture plate was taken out, and the probe plate was inserted into the cell culture plate and placed into the instrument for detection.

2.12. Data analysis and statistics

All experiments were performed in triplicate. Values are expressed as the mean of average ± standard deviation. The statistical differences were evaluated by using ANOVA (one-way ANOVA and two-way ANOVA). Differences with a value of $P < 0.05$ were considered statistically significant. A Dunnett's test was used for post hoc analysis when required.

3. Results

3.1. Preparation and characterization of Blank-NPs, SRM-NPs and PTX-NPs

We prepared a nano-delivery system by using lipid-soluble polymer (3S-PLGA) as a carrier. The size, stability, cytocompatibility and drug release kinetics of NPs were characterized (Fig. 1&2). The particle sizes of Blank-NPs, SRM-NPs and PTX-NPs were (204.7 ± 1.1) nm, (214.3 ± 0.6) nm and (216.9 ± 0.6) nm, the PDI value was (0.099 ± 0.008), (0.098 ± 0.022) and (0.129 ± 0.046), and the surface potential was -(12.05 0.35) mV, -(12.10 ± 0.14) mV and -(14.35 ± 0.21) mV (Fig. 1 A). For 21 days, the sizes of Blank-NPs, SRM-NPs and PTX-NPs were tested. Almost no change in particle size indicated that NPs were relatively stable (Fig. 1 B). Both SRM-NPs and PTX-NPs showed similar drug release kinetics which manifested as a 21-day slow release (Fig. 1C). Under TEM, three kinds of NPs were all spherical (Fig. 1 D). In addition, drug loading of SRM-NPs and PTX-NPs were (21.8 ± 0.8) % and (17.0 ± 0.7) % respectively and the encapsulation rate of them were (98.7 ± 0.0) % and (99.5 ± 0.1) % respectively.

Under different microenvironments of normal and hypoxia, NPs successfully entered EC and SMC through endocytosis and the cell viability exceeded 75%, showing good cytocompatibility (Fig. 2 A, a & B, a). NPs could also escape from lysosome through the interaction with lysosomal membrane, which will help to improve the bioavailability of sirolimus and paclitaxel (Fig. 2 A, b & B, b). The phagocytic and release behavior of SRM-NPs and PTX-NPs was consistent. Therefore, it's appropriate to compare the efficacy of sirolimus and paclitaxel basing this NPs and further explore their mechanism.

3.2. The curative effect of SRM-NPs on Chinese Experimental Mini-pigs

In previous studies, Konstantinos spargias et al. Showed that paclitaxel can inhibit the expression of proliferating cell nuclear antigen (PCNA) and reduce vascular stenosis [16]. Our previous studies have shown that paclitaxel can inhibit neointimal hyperplasia more effectively by delivering paclitaxel through nano delivery system [17]. Similarly, we examined the inhibitory effects of sirolimus on vascular stenosis and cell proliferation (Fig. 3). Degree of stenosis of SRM-NPs group was (23.4% ± 5.35) %, in contrast to (46.07 ± 18.33) % of saline group ($P < 0.01$) and (39.32% ± 9.91) % of SRM group ($P < 0.05$). The proliferative index of SRM-NPs group was 0.39 ± 0.03, in contrast to 0.89 ± 0.18 and 0.78 ± 0.20 of saline group and SRM ($P < 0.05$). In SRM-NPs group, the expression of PCNA was (29.32% ± 10.1) %, which compared with (47.9% ± 15.4) % of SRM group ($P < 0.01$) and (66.7% ± 13.3) % of saline group respectively ($P < 0.05$). Comparatively speaking, the SRM-NPs group had mild intimal hyperplasia and large residual vascular lumen area. PCNA, as proliferative nuclear antigen, was significantly more expressed in the normal saline group, Blank-NPs group and SRM group than in SRM-NPs group. The results showed that sirolimus could inhibit vascular stenosis and cell proliferation successfully. After sirolimus was

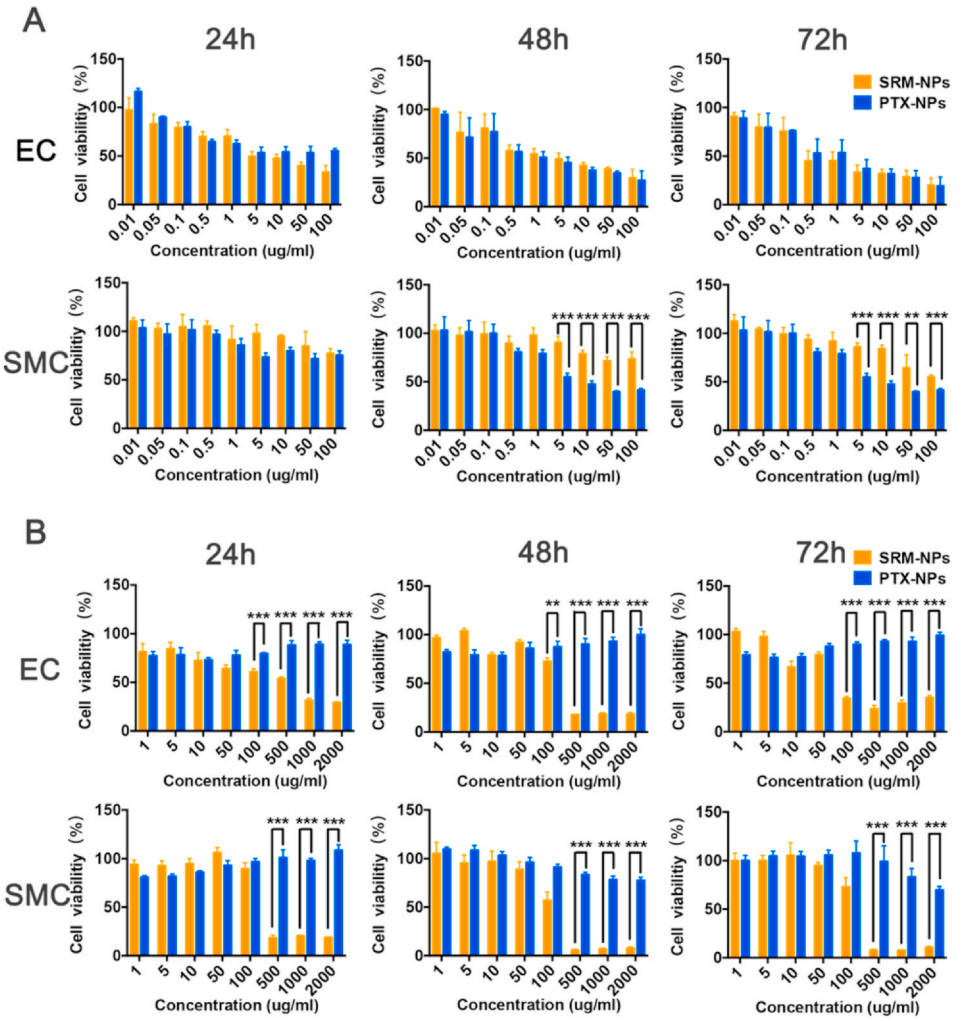

Fig. 4. Comparison of cell proliferation inhibition under normoxia and hypoxia. At 24 h, 48 h and 72 h, the inhibitory effects of SRM-NPs and PTX-NPs on EC and SMC proliferation were compared under normoxia (A) or hypoxia (B) within 24 h–72 h. The results suggested that paclitaxel seemed only inhibited the proliferation of normoxic cells. On the contrary, sirolimus-eluting stents could inhibit the proliferation of both hypoxic and normoxic cells.

delivered by nano delivery system, the ability of inhibiting vascular stenosis and cell proliferation was enhanced.

3.3. Comparison of cell proliferation inhibition under normoxia and hypoxia

Both sirolimus and paclitaxel used as anti-proliferative stent drugs in the treatment of restenosis, but the effects were different [18]. For a deeper understanding of treatment differences, MTT assay was performed to detect cell proliferation and we have carried out the following exploration. Firstly, under normoxia, cell viability was measured after EC and SMC were treated with different concentrations of SRM-NPs and PTX-NPs (Fig. 4A), ranging from 0.3 to 3000 ng/mL for 24 h, 48 h and 72 h. The results showed that both SRM-NPs and PTX-NPs could anti-proliferation on cells in a time- and dose-dependent way under normoxia. Then, considering that most studies ignored the drug resistance of cells caused by hypoxic microenvironment of atherosclerosis [19], further comparisons had been made under hypoxia in this study. In further experiments, under the same NP-concentration and treatment time, both EC and SMC showed drug resistance to SRM-NPs and PTX-NPs under hypoxia. But surprisingly, when we increased the doses of NPs, SRM-NPs exhibited time- and dose-dependent anti-proliferative effects on hypoxic EC and SMC (containing 0.03–60 μg/mL sirolimus), while PTX-NPs couldn't inhibit cell proliferative at the same concentration (Fig. 4 B). The differences between SRM-NPs and PTX-NPs were striking in this situation (***$P < 0.001$).

It can be seen from the results that PTX-NPs were slightly superior to SRM-NPs in anti-proliferation ability of normoxic cells. This is in line with previous results that paclitaxel has a better pro-apoptotic effect on normoxic cells than sirolimus [20]. However, this study suggested that compared with SRM-NPs, anti-proliferative effect of PTX-NPs on hypoxic cells was noticeably weakened. This may suggest that using of sirolimus is superior to paclitaxel in vascular restenosis.

3.4. Comparison of HIF-1α expression under hypoxia

The main mechanism of cells dealing with hypoxia is stabilization and overexpression of hypoxia inducible factor 1 (HIF-1) [21–23]. HIF-1 can target multiple genes and regulate cell metabolism, which play a key role in the development of atherosclerosis by acting on the cell-specific responses of EC and SMC [24–26].

HIF-1 is composed of HIF-1α and HIF-1β. HIF-1α is a functional unit regulated and controlled by oxygen content, while HIF-1β is a structural unit unaffected under hypoxia. HIF-1 α regulates cells to adapt to hypoxia environment by activating genes to change energy metabolism [27,28]. Therefore, we explored the effects of SRM-NPs, PTX-NPs and Blank-NPs on HIF-1 expression in hypoxic cells. Firstly, the results showed that Blank-NPs had no effect of the expression of HIF-1α under hypoxia. Secondly, expression of HIF-1α in SRM-NPs group was significantly weakened, which means that SRM-NPs could inhibit the

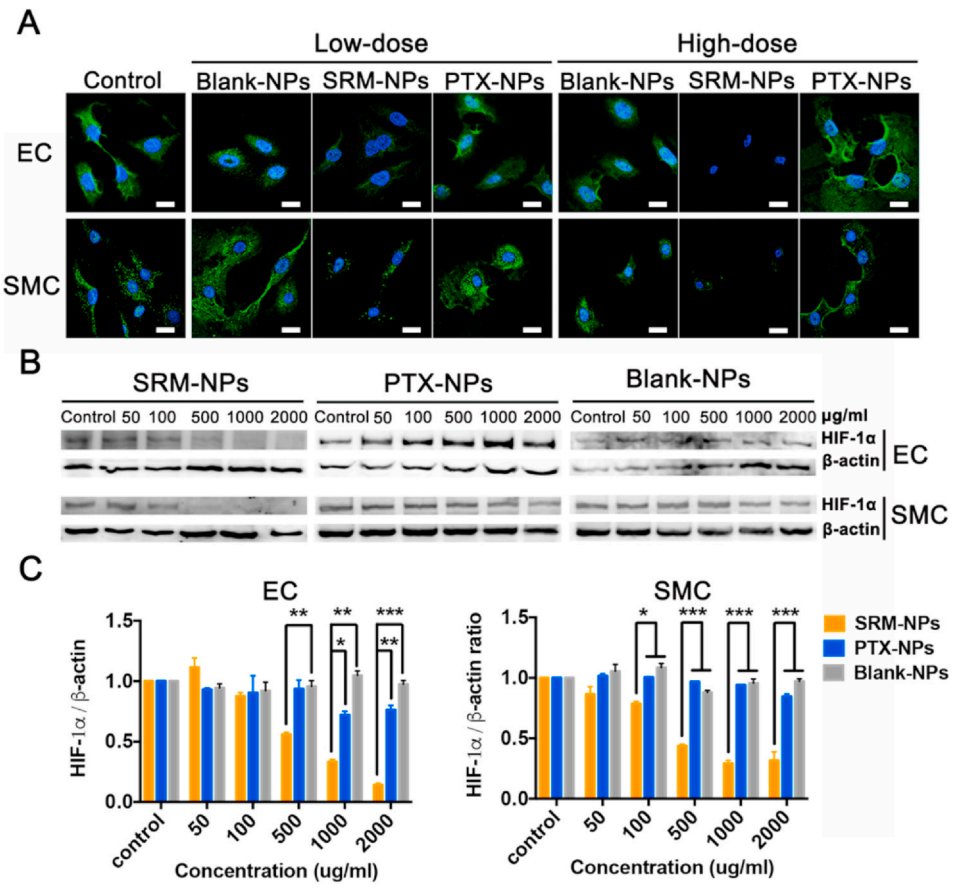

Fig. 5. Effect on HIF-1α expression of SRM-NPs and PTX-NPs under normoxia. The expression of HIF-1α was detected by cellular immunofluorescence assay and Western blot. The inhibition of HIF-1α expression by Blank-NPs, SRMS -NPs and PTX-NPs at low-dose (100 μg/mL) and high-dose (1000 μg/mL) was detected by laser confocal microscopy. (A), at various concentrations (50, 100, 500, 1000, 2000 μg/mL) was detected by Western blot (B) and quantified by Image J software(C). (A)The white bars represent 20 μm, blue stands for DAPI and green represents HIF-1α. Our results suggested that PTX-NPs couldn't inhibit the expression of HIF-1α, but RPM-NPs can achieve this. Cellular immunofluorescence assay also supported similar conclusion. (For interpretation of the references to color in this figure legend, the reader is referred to the Web version of this article.)

expression of HIF-1α in hypoxic EC and SMC. However, PTX-NPs could hardly inhibit the expression of HIF-1α at the same concentration under hypoxia (Fig. 5B&C). Cellular immunofluorescence assay also supported similar conclusion (Fig. 5A).

3.5. Comparison of glycolysis under hypoxia

When HIF-1α is up-regulated with low and stable oxygen content, the glycolysis in hypoxic cells changes, which allows cells to maintain ATP synthesis under hypoxic conditions [29–32]. Thus, the glycolysis regulated by HIF-1α is very important for proliferation of hypoxic cells in atherosclerotic sites. Basing on this, we also explored the effects of Control, SRM-NPs, PTX-NPs and Blank-NPs groups on glycolysis of EC and SMC under hypoxia.

The experiment firstly created a state in which cells almost stopped metabolizing. The medium contained only a little amount of glutamine to maintain cell survival. After the first injection of glucose, the cells began to metabolize glucose (including aerobic oxidation and anaerobic glycolysis). The result showed that the glycolysis process treated by SRM-NPs in SMC and EC was weaker than the other three groups, and the inhibitory effect of SRM-NPs increased when dose increased (Fig. 6). The second injection of oligomycin inhibited mitochondrial aerobic oxidation, and the energy supply of cells was completely converted to glycolysis, which showed the maximum glycolysis capacity of cells. It could be seen that the glycolysis processes of control, PTX-NPs and Blank-NPs groups were promoted after oligomycin was added, but the promotion effects were not strong. This may due to the fact that the construction of hypoxia environment inhibited most of the aerobic oxidation process (Fig. 6). It's well known that glycolysis provides ATP for cells to survive in hypoxia. Sirolimus could inhibit the proliferation of hypoxic cells by inhibiting glycolysis, while paclitaxel couldn't. This result may also indicate that sirolimus had an advantage over paclitaxel in prevention of restenosis. For the convenience of understanding, the relevant mechanism of this study was also shown in Fig 7.

4. Discussion

Decrease of oxygen tension in tissues plays an important role in the progression of atherosclerosis [33]. With the development of atherosclerosis, the arterial wall becomes thicker and the diffusion of oxygen to intima is reduced. In fact, in both human and animal models, advanced atherosclerotic plaques show areas of severe hypoxia [34,35]. However, most of the mechanism research seems to ignore the change of oxygen microenvironment, which is obviously inappropriate. Therefore, we attempted to compare the effects of sirolimus and paclitaxel on hypoxic cell proliferation and explore their mechanism.

In atherosclerosis, the angiogenesis of atherosclerotic plaque is related to the progression and instability of atherosclerotic plaque [36]. Neovascularization mainly occurred in the deep part of the thickened intima and media, and associated cells are hypoxic. With the increase of plaque hypoxia, microvessel density increased [37]. It is of great significance to inhibit angiogenesis in plaque to stabilize plaque and inhibit plaque rupture. Therefore, microvascular-related EC and SMC were used as cell models in this study.

In addition, we established the porcine carotid arty injury model to evaluate the effects of SRM-NPs on vascular stenosis, proliferation index and PCNA expression. The results showed that SRM-NPs could successfully reduce the loss of vascular lumen area, which may be related to the inhibition of PCNA expression. Sirolimus has a better therapeutic effect after being delivered by nano delivery system.

Afterwards, we compared the effects of sirolimus and paclitaxel on the proliferation of hypoxic and normoxic cells. The results showed that PTX-NPs seemed to have a stronger inhibitory effect under normoxic conditions. In fact, previous studies have shown that sirolimus and

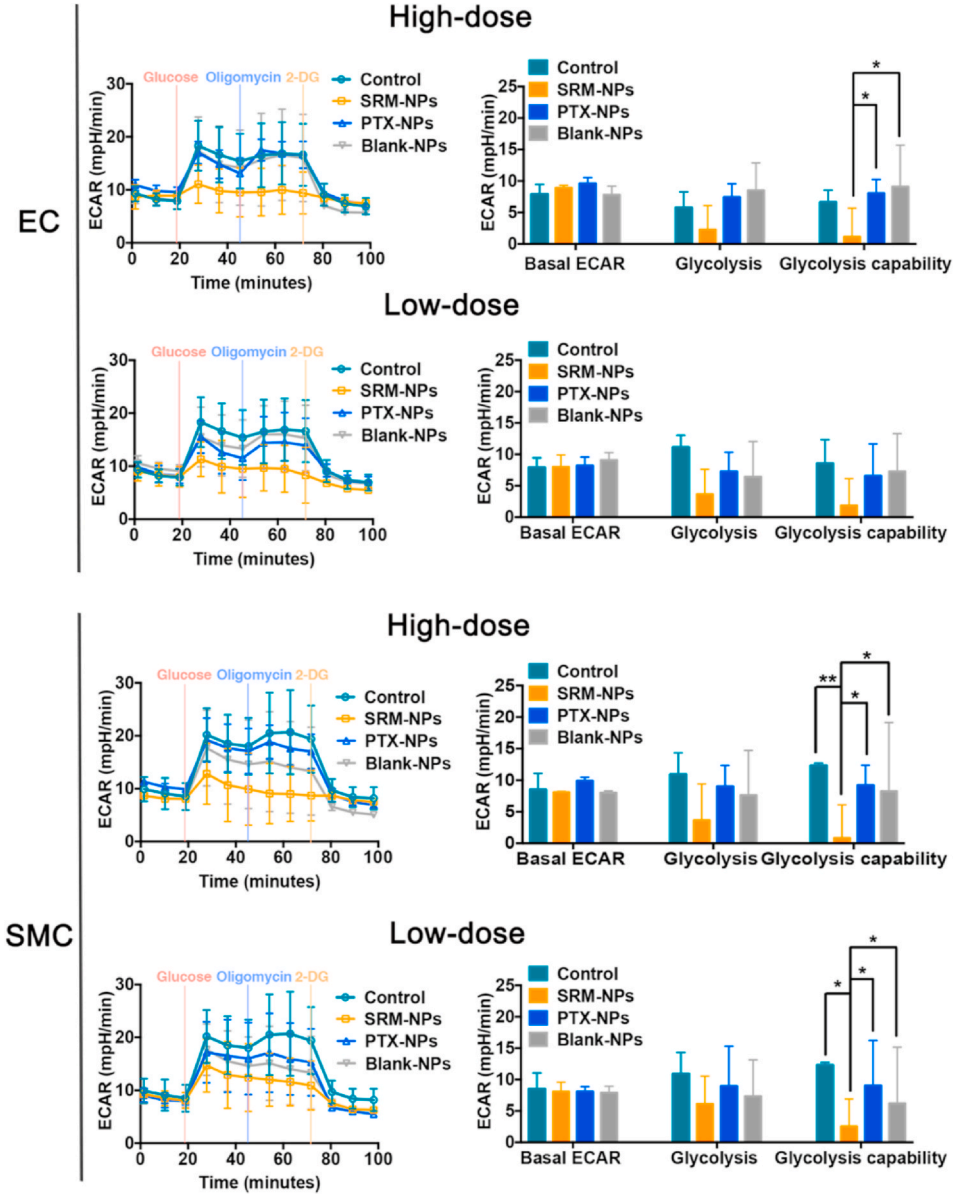

Fig. 6. Effects on cell glycolysis of Blank-NPs, SRMS -NPs and PTX-NPs under hypoxia. The effects of Blank-NPs, SRMS -NPs and PTX-NPs on EC, SMC glycolysis at low-dose (100 μg/mL) and high-dose (1000 μg/mL) were detected by real-time hippocampal energy metabolism analyzer X24. Among them, the left column is real-time measurement curve of cell glycolysis metabolism, and the right column is quantitative analysis result. Wave software was used for quantitative analysis. The results showed that glycolysis ability of SRM-NPs group was lower than that of both Blank-NPs and PTX-NPs groups at high doses. In addition, there was no significant difference in glycolysis among PTX-NPs, Blank-NPs and Control groups.

paclitaxel had similar inhibitory effects on the proliferation of normoxic EC and SMC, but paclitaxel had stronger pro-apoptotic effects [38]. The inhibitory effect of SRM-NPs on the proliferation of hypoxic cells was time- and dose-dependent, while the anti-proliferation effect of PTX NPs was significantly weakened. Although the effect of paclitaxel in this study was weakened, paclitaxel may still inhibit the proliferation of hypoxia cells after increasing the dose. However, this will lead to increased systemic toxicity of paclitaxel, even life-threatening. This may also explain why paclitaxel has such a narrow treatment window. It could be seen that the change of oxygen-containing microenvironment seems to have a significant effect on the anti-proliferation ability of drugs. After observing the superiority of sirolimus in inhibiting hypoxic cell proliferation, we further explored the possible molecular mechanism of this phenomenon.

Cells deal with hypoxia by stabilizing transcription factors known as hypoxia inducible factor (HIF-1). At low oxygen levels, HIF-1 enters the nucleus to drive target gene expression. Among hundreds of verified HIF-1 target genes, there are multiple genes that regulate cell metabolism. Over-expressed HIF-1 could lead to the proliferation of SMC, and the proliferation rate of SMC cultured at low oxygen (3% O_2) was 113.6% higher than that under normal conditions [39]. HIF-1 also leads to gene transcriptional induction in EC under hypoxia, such as Glut-1, VEGF, iNOS, etc., so that cells can survive and proliferate in hypoxic environment [40]. Therefore, the inhibition of HIF-1 expression by drugs would be helpful for anti-proliferation. The results of this study showed that RPM NPs could significantly inhibit HIF-1 α expression in ECs and SMCs in a dose-dependent manner, while PTX NPs could hardly inhibit HIF-1a expression at the same concentration. This may indicate the possible reason that PTX-NPS could not inhibit cell proliferation under hypoxia.

Blood flow characteristics of atherosclerotic lesions change from unidirectional flow to disturbed flow. Disturbed flow is related to lower shear stress, which can improve cell metabolism and reduce the integrity of vascular barrier [41]. Studies have shown that low shear stress activates specific genes and regulates cell processes: hypoxia and glycolysis [42]. What's more, further molecular analysis showed that HIF-1 promoted glycolysis and the increase of glycolysis sometimes cause vascular inflammation [43].

Increased glycolysis may cause vascular inflammation and cellular mitochondrial dysfunction, and with the enhancement of glycolysis, cell proliferation is promoted [44]. The inhibition of glycolysis by anti-proliferative drugs will help to limit the complex progress of

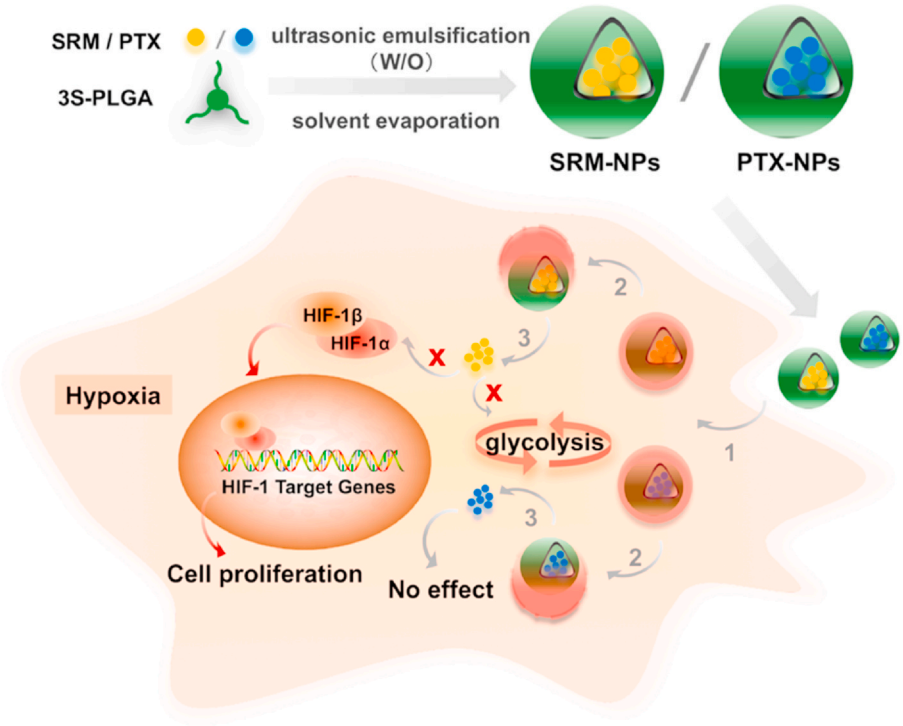

Fig. 7. Schematic diagram of mechanism. Sirolimus and paclitaxel were delivered by 3s-PLGA nano-delivery system and lysosomal escape was achieved. After that, sirolimus successfully inhibited the expression of HIF-1α and glycolysis, cell proliferation was inhibited, while paclitaxel could not achieve a significant inhibitory effect. (Step1 stands for cellular uptake, Step 2 stands for lysosome escape, Step 3 stands for disassembling, Red Cross stands for inhibition and red arrow stands for Inhibited pathway in EC and SMC). (For interpretation of the references to color in this figure legend, the reader is referred to the Web version of this article.)

atherosclerotic anoxic sites. The results of this study showed that SRM-NPs inhibited glycolysis of hypoxia EC and SMC, while PTX-NPS did not. This may be due to the inhibitory effect of SRM-NPS on HIF-1.

Therefore, according to the experimental results, the reason why sirolimus-eluting stent gradually replaced paclitaxel eluting stent may be related to the stronger anti-proliferation effect of sirolimus on hypoxic cells than paclitaxel. Similarly, paclitaxel is the main drug currently used in drug coating balloons. In the future, sirolimus may be used instead of paclitaxel in drug coated balloon to obtain better therapeutic effect. There are metabolic abnormalities in the cells of hypoxic area of atherosclerosis. We compared the therapeutic effect of paclitaxel and sirolimus on hypoxia cells by constructing hypoxia microenvironment in vitro. However, there are still significant differences between the hypoxic cells in vitro and in vivo. In this study, the relationship between the dose gradients of NP-based sirolimus and paclitaxel under normoxia or hypoxia and their therapeutic effects was clarified. However, due to the influence of carrier polymer, diffusion rate, internal environmental interference and individual differences, the dose of this experiment may not directly correspond to the dose of stent or balloon drug. At present, although we have opened up a new field of vision in comparing the differences between sirolimus and paclitaxel, more researches are still needed to provide complete theoretical support for the selection of vascular restenosis. It is hoped that this study will inspire more thinking and research, and contribute to the treatment of vascular restenosis in the future.

5. Conclusion

In conclusion, sirolimus has a stronger anti-proliferation effect on atherosclerosis related hypoxic cells than paclitaxel, which may make sirolimus more suitable for the treatment of vascular restenosis. Therapeutic advantage of sirolimus seems related to inhibitions of HIF-1α expression and glycolysis. This study aims to further explore the anti-proliferation mechanism of sirolimus and paclitaxel in vitro and hope to stimulate more thinking and research of drug selection to promote the and further treatment of vascular restenosis.

CRediT authorship contribution statement

Youlu Chen: Methodology, Validation, Formal analysis, Roles, Writing - original draft. **Yong Zeng:** Methodology, Validation, Formal analysis, Roles, Writing - original draft. **Xiaowei Zhu:** Investigation, Resources. **Lifu Miao:** Investigation, Resources. **Xiaoyu Liang:** Formal analysis, Data curation. **Jianwei Duan:** Investigation, Resources. **Huiyang Li:** Investigation, Resources. **Xinxin Tian:** Formal analysis, Data curation. **Liyun Pang:** Writing - review & editing, Supervision. **Yongxiang Wei:** Writing - review & editing. **Jing Yang:** Conceptualization, Writing - review & editing, Project administration, Funding acquisition.

Declaration of competing interest

The authors declare that they have no known competing financial interests or personal relationships that could have appeared to influence the work reported in this paper.

Acknowledgments

The authors are grateful to the financial support from the National Natural Science Foundation of China of China (31771097), Tianjin Research Program of Application Foundation and Advanced Technology (17JCZDJC3070), AMS Innovation Fund for Medical Sciences (2017-I2M-1–016) and Tianjin Innovation and Promotion Plan Key Innovation Team of Immunoreactive Biomaterials.

References

[1] W. Sun, C. Liu, Q. Chen, N. Liu, Y. Yan, B. Liu, SIRT3: a new regulator of cardiovascular diseases, Oxidative Medicine & Cellular Longevity 2018 (4) (2018) 1–11.
[2] T.J. Hong, H.W. Lee, J.H. Choi, J.C. Choi, J. Ahn, J.S. Park, et al., Comparison of long term clinical outcomes between bare metal stent versus different types of drug eluting stents for treatment of acute myocardial infarction, Atherosclerosis 263 (2017) e155–e156.
[3] P. Mortier, M. De Beule, G. Carlier, R. VanImpe, B. Verhegghe, P. Verdonck, Numerical study of the uniformity of balloon-expandable stent deployment, J. Biomech. Eng. 130 (2) (2008) 021018.
[4] M. Nakagawa, T. Ohno, R. Maruyama, M. Okubo, A. Nagatsu, M. Inoue, et al.,

Sesquiterpene lactone suppresses vascular smooth muscle cell proliferation and migration via inhibition of cell cycle progression, Biol. Pharmaceut. Bull. 30 (9) (2007) 1754–1757.
[5] S.O. Marx, H. Totary-Jain, A.R. Marks, Vascular smooth muscle cell proliferation in restenosis, Circulation. Cardiovascular interventions 4 (1) (2011) 104.
[6] G.W. Stone, S.G. Ellis, D.A. Cox, J. Hermiller, C. O'Shaughnessy, J.T. Mann, M. Turco, R. Caputo, P. Bergin, J. Greenberg, J.J. Popma, M.E. Russell, Taxus-IV Investigators, One-year clinical results with the slow-release, polymer-based, paclitaxel-eluting TAXUS stent: the TAXUS-IV trial, Circulation 109 (16) (2004 Apr 27) 1942–1947.
[7] J. Kong, P. Liu, X. Fan, J. Wen, Z. Ye, Long-term outcomes of paclitaxel-eluting versus sirolimus-eluting stent for percutaneous coronary intervention: a meta-analysis, Journal of the College of Physicians & Surgeons Pakistan Jcpsp 27 (7) (2017 Jul) 432–439.
[8] B. Senst, A. Goyal, J. Borger, Drug eluting stent (DES) compounds, StatPearls, 2020 Treasure Island (FL).
[9] Manabu Kaneko, Hiroaki Nozawa, Nelson H. Tsuno, et al., Abstract 2819: temsirolimus inhibits colon cancer growth in vitro and in vivo, Canc. Res. 72 (8 Supplement) (2012) 2819-2819.
[10] Or Bida, Moriah Gidoni, Diana Ideses, et al., A novel mitosis-associated lncRNA, MA-linc1, is required for cell cycle progression and sensitizes cancer cells to Paclitaxel, Oncotarget 6 (29) (2015) 27880–27890.
[11] Mateo J, Izquierdo-Garcia D, Badimon J, Fayad A, Fuster V, Noninvasive assessment of hypoxia in rabbit advanced atherosclerosis using 18f-fluoromisonidazole positron emission tomographic imaging. Circulation Cardiovascular Imaging, 7(2), 312-320..
[12] T. Jain, E.A. Nikolopoulou, Q. Xu, A. Qu, Hypoxia inducible factor as a therapeutic target for atherosclerosis, Pharmacol. Therapeut. 183 (2018) 22–33.
[13] W. Chen, T.C. Habraken, W.E. Hennink, R.J. Kok, Polymer-free drug-eluting stents: an overview of coating strategies and comparison with polymer-coated drug-eluting stents, Bioconjugate Chem. 26 (7) (2015) 1277–1288.
[14] D. Piraino, Paclitaxel eluting balloon and sirolimus eluting balloon, many weapons against a common enemy: the in-stent restenosis, Int. J. Cardiol. 242 (2017) 4.
[15] S. Wang, R. Su, S. Nie, M. Sun, J. Zhang, D. Wu, et al., Application of nanotechnology in improving bioavailability and bioactivity of diet-derived phytochemicals, JNB (J. Nutr. Biochem.) 25 (4) (2014) 363–376.
[16] T.H. Wang, H.S. Wang, Y.K. Soong, Paclitaxel-induced cell death: where the cell cycle and apoptosis come together, Cancer 88 (2000) 2619–2628.
[17] V. Kasivisvanathan, J. Shalhoub, C.S. Lim, A.C. Shepherd, A. Thapar, A.H. Davies, Hypoxia-inducible factor-1 in arterial disease: a putative therapeutic target, Curr. Vasc. Pharmacol. 9 (3) (2011) 333–349.
[18] C.S. Lim, S. Kiriakidis, A. Sandison, E.M. Paleolog, A.H. Davies, Hypoxia-inducible factor pathway and diseases of the vascular wall, J. Vasc. Surg. 58 (1) (2013) 219–230.
[19] Guo-Hua Fong, Potential contributions of intimal and plaque hypoxia to atherosclerosis, Curr. Atherosclerosis Rep. 17 (6) (2015) 32.
[20] E. Marsch, J.C. Sluimer, M.J.A.P. Daemen, Hypoxia in atherosclerosis and inflammation, Curr. Opin. Lipidol. 24 (5) (2013) 1.
[21] C. Hao, H. Duan, S. Li, Effect on the expression of VEGF and HIF-1 alpha in atherosclerosis rat myocardial with oral HSP60 (618.8), Faseb. J. 28 (1_supplement) (2014) 618.8.
[22] A. Aarup, T.X. Pedersen, N. Junker, C. Christoffersen, E.D. Bartels, M. Madsen, et al., Hypoxia-inducible factor-1α expression in macrophages promotes development of atherosclerosis, Arterioscler. Thromb. Vasc. Biol. 36 (9) (2016) ATVBAHA.116.307830.
[23] G.L. Semenza, Hypoxia-inducible factor 1 (HIF-1) pathway, Sci. STKE 2007 (407) (2007) cm8-cm8.
[24] A. Aarup, T.X. Pedersen, N. Junker, C. Christoffersen, L.B. Nielsen, Hypoxia-inducible factor-1α expression in macrophages promotes development of atherosclerosis, Arterioscler. Thromb. Vasc. Biol. 36 (9) (2016) 1782–1790.
[25] X. Peng, F. Gong, Y. Chen, Y. Jiang, J. Liu, M. Yu, et al., Autophagy promotes paclitaxel resistance of cervical cancer cells: involvement of Warburg effect activated hypoxia-induced factor 1-α-mediated signaling, Cell Death Dis. 5 (8) (2014) e1367.
[26] M. Wangpaichitr, J. Maher, M. Kurtoglu, N. Savaraj, T. Lampidis, Inhibition of mTOR activity potentiates 2-DG-induced cell death in hypoxic cells via down-regulation of HIF-1α, Canc. Res. 67 (2007).
[27] M.C. Brahimi-Horn, J. Chiche, Jacques Pouysségur, Hypoxia signalling controls metabolic demand, Curr. Opin. Cell Biol. 19 (2) (2007) 223–229.
[28] Y. Zhou, F. Tozzi, J. Chen, et al., Intracellular ATP Levels Are a Pivotal Determinant of Chemoresistance in Colon Cancer Cells 72 (2012), pp. 304–314 1.
[29] James B. Hermiller, Drug-eluting stents in the management of coronary artery disease: implications for payors and hospitals, Dis. Manag. Health Outcome 13 (1) (2005) 1–7.
[30] S.M. Shwarz, Prospective series: cell adhesion in vascular biology. Smooth muscle migration in atherosclerosis and restenosis, J. Clin. Invest. 99 (1997).
[31] A.D. Levin, N. Vukmirovic, C.W. Hwang, et al., Specific binding to intracellular proteins determines arterial transport properties for rapamycin and paclitaxel, Proc. Natl. Acad. Sci. U.S.A. 101 (25) (2004) 9463–9467.
[32] J. Eduardo Sousa, Patrick W. Serruys, Marco A. Costa, New frontiers in cardiology drug-eluting stents: part I, Circulation 107 (17) (2003) 2274–2279.
[33] S.A. Carter, Effects of ambulation on foot oxygen tension in limbs with peripheral atherosclerosis, Clin. Physiol. 16 (3) (2010) 199–208.
[34] S. Parathath, Y. Yang, S. Mick, A. Fisher, Hypoxia in murine atherosclerotic plaques and its adverse effects on macrophages, Trends Cardiovasc. Med. 23 (3) (2013) 80–84.
[35] X. Nie, J. Randolph, A. Elvington, N. Bandara, A. Zheleznyak, J. Gropler, et al., Imaging of hypoxia in mouse atherosclerotic plaques with 64cu-atsm, Nucl. Med. Biol. 43 (9) (2016) 534–542.
[36] L. Mehta, P. Mathur, S. Dhalla, Biochemical Basis and Therapeutic Implications of Angiogenesis || Trials of Angiogenesis Therapy in Patients with Ischemic Heart Disease, (2017), pp. 393–421, https://doi.org/10.1007/978-3-319-61115-0 (Chapter 18).
[37] Sanne W, Aryan V, Ilze B, Quax A, Jan G, De M, et al, Mast cells in human carotid atherosclerotic plaques are associated with intraplaque microvessel density and the occurrence of future cardiovascular events. Eur. Heart J. (48), 3699-3706.
[38] W. Rainer, S. Albert, K. Adnan, Sirolimus and paclitaxel on polymer-based drug-eluting stents: similar but different, J. Am. Coll. Cardiol. 47 (4) (2006).
[39] W. Wang, P. Wang, S. Li, et al., Methylprednisolone inhibits the proliferation and affects the differentiation of rat spinal cord-derived neural progenitor cells cultured in low oxygen conditions by inhibiting HIF-1Î ± and Hes1 in vitro, Int. J. Mol. Med. 34 (3) (2014) 788–795.
[40] Shaolian Song, Xiaoyan Xiao, Dan Guo, et al., Protective effects of Paeoniflorin against AOPP-induced oxidative injury in HUVECs by blocking the ROS-HIF-1α/VEGF pathway, Phytomedicine 34 (2017) 115–126.
[41] Ene-Iordache Bogdan, Cattaneo Luca, Dubini Gabriele, et al., Effect of anastomosis angle on the localization of disturbed flow in 'side-to-end' fistulae for haemodialysis access, Nephrol. Dial. Transplant. (4) (2012) 4.
[42] S. Feng, N. Bowden, M. Fragiadaki, et al., Mechanical Activation of Hypoxia-Inducible Factor 1α Drives Endothelial Dysfunction at Atheroprone Sites, Arteriosclerosis Thrombosis & Vascular Biology 37 (11) (2017) 2087–2101. ATVBAHA.117.309249.
[43] W. Wang, P. Wang, S. Li, et al., Methylprednisolone inhibits the proliferation and affects the differentiation of rat spinal cord-derived neural progenitor cells cultured in low oxygen conditions by inhibiting HIF-1 α ± and Hes1 in vitro, Int. J. Mol. Med. 34 (3) (2014) 788–795.
[44] Shaolian Song, Xiaoyan Xiao, Dan Guo, et al., Protective effects of Paeoniflorin against AOPP-induced oxidative injury in HUVECs by blocking the ROS-HIF-1α/VEGF pathway, Phytomedicine 34 (2017) 115–126.